Pergamon

Cement and Concrete Research 30 (2000) 1517–1525

CEMENT AND CONCRETE RESEARCH

Review

Mercury porosimetry
An inappropriate method for the measurement of pore size distributions in cement-based materials

Sidney Diamond*

School of Civil Engineering, Purdue University, West Lafayette, IN 47907-1284, USA

Received 3 January 2000; accepted 17 July 2000

Abstract

The conditions that must be met for mercury intrusion porosimetry (MIP) measurements to provide valid estimates of the pore size distribution of porous solids are reviewed. Evidence is presented indicating that these conditions are not satisfied in cement-based systems. In cement-based systems, nearly all of the mercury intrusion is held up until pressure corresponding to the threshold diameter is reached; subsequently, large and small pores are filled indiscriminately. Air voids, in sizes up to several hundred micrometers, are present in most pastes in substantial volume, unless the pastes were mixed under vacuum; these air voids are also not intruded until the threshold pressure is reached, and are recorded as fine (ca. 0.1 μm) pores. It is concluded that MIP measurements are useful only to provide threshold diameters and intrudable pore space measurements, which can serve as comparative indices for the connectivity and capacity of the pore systems in hydrated cements. MIP measurements should be abandoned as measures of the actual pore sizes present.

Keywords: Mercury porosimetry; Pore size distribution; Image analysis; Backscattered electron imaging; Microstructure

1. Introduction

For many years, it has been customary in cement research to evaluate pore size distributions in cement pastes, mortars, and occasionally concretes, using mercury intrusion porosimetry (MIP). A large number of papers, perhaps several thousand, have appeared containing purported pore size distributions of such hydrated cement materials based on MIP. Such papers continue to appear with regularity, recent examples in the present journal alone including those of Khatib and Wild [1], Zhang [2], Bagel [3], Kanna et al. [4], Willis et al. [5], Loukili et al. [6], Cook and Hover [7], and Puerta et al. [8]. Cook and Hover [7] presented an extensive library of MIP curves of pastes of systematically varying age and w:c ratio.

It is the intent of the present paper to marshal evidence indicating that MIP-derived pore size distributions do not, in fact, provide even approximately correct measures of the sizes of the pores that actually exist in the systems being measured.

2. Physical basis of mercury intrusion measurements

Mercury intrusion measurements are extremely simple in principle, although a number of experimental complications need to be considered. In the usual procedure, a small specimen is first dried to empty the pores of any existing fluid. It is then weighed, transferred to a chamber, which is then evacuated, and mercury is introduced to surround the specimen. Since mercury does not wet cementitious solids spontaneously, it does not intrude into empty pores unless pressure is applied. Pressure in progressive increments is then applied to the mercury, and the intrusion of mercury at each step is monitored. The set of pressure steps and corresponding volumes intruded provides the basic data for pore size distribution calculations. An example of such a set of raw data is provided in Fig. 1, for a 14-day-old w:c 0.35 paste. The reproducibility of the experiment is extremely high; the

* Tel.: +1-765-494-5016; fax +1-765-496-1364.
E-mail address: diamond@ecn.purdue.edu (S. Diamond).

0008-8846/00/$ – see front matter
PII: S0008-8846(00)00370-7

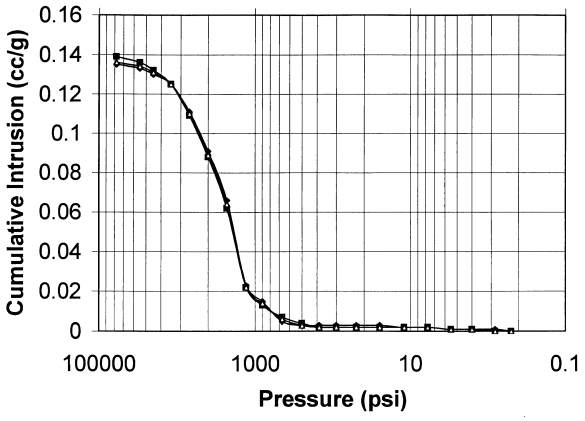

Fig. 1. Cumulative mercury intrusion vs. pressure curve for a 14-day-old w:c 0.35 cement paste.

results of three separate replicate trials are actually plotted in the figure.

However, the mercury intrusion data by itself provides no information whatsoever on the distribution of sizes of pores in the specimen. For such information to be generated, an appropriate model must first be invoked.

The usual model is that of a system of cylindrical pores each of which is entirely and equally accessible to the outer surface of the specimen, and thus to the surrounding mercury. For porous systems that conform to such a model, the well-known Washburn equation may be properly applied to estimate the diameter of cylindrical pores intruded at each pressuring step, viz:

$$d = -4g\cos\theta/P \quad (1)$$

where d is the diameter of the cylinder being intruded, g is the surface tension of mercury, θ is the contact angle of mercury on the solid, and P is the applied pressure.

There is no distinction in the model between intrusion into a single long, continuous cylinder or intrusion into a multitude of shorter cylinders of the same diameter, as long as they are all open to the outer surface.

Very few real materials actually fulfill the requirements of the model. One that does is a type of membrane laboratory filter that is manufactured so as to contain cylindrical pores of a specified diameter; such filters allow fluids to pass but positively filter off particles larger than the specified diameter.

A cement material that fulfills these requirements can be created experimentally by drilling parallel cylindrical holes through disks of hardened cement paste. The diameters of such drilled holes can be measured by optical microscopy. The Washburn equation relates the pressure at which these cylindrical pores are intruded by mercury to their diameter. Shi and Winslow [9] used this technique to indirectly measure contact angles of mercury on various cement pastes.

However, it has become increasingly apparent that the intrinsic pores in hydrated cement systems fail to conform to the requirements of the model. The nature of this failure is such that the putative pore size distribution calculated from the Washburn equation from MIP data departs enormously from reality, most pores being reported one or two orders of magnitude smaller than they actually are. Furthermore, it appears that the appearance of the MIP pore size distribution curve generated by application of the Washburn equation to MIP data is an artifact that reflects the physics of how mercury intrudes into the paste and is not controlled by the actual sizes of the pores present.

3. Pores in hydrated cement systems: pore shapes

As mentioned previously, the Washburn model used to convert mercury intrusion data, such as that of Fig. 1, into pore size distribution curves invokes two distinct assumptions: (1) that pores are cylindrical, and (2) that they are entirely and equally accessible to the outer surface of the specimen. The latter requirement is far more important, but the former is easier to explore, and will be treated first.

Fig. 2a is a representative backscatter SEM view of a 7-day-old w:c 0.45 hardened cement paste. The figure is a digitized image consisting of 409,600 individual pixels, the brightness of each of which is reproduced at a specific gray level on a scale between 0 and 255. The gray level of each pixel reflects the electron backscatter effectiveness of the particular solid occupying its location. Pores in cement pastes as normally prepared for backscatter SEM are ordinarily filled with hardened epoxy resin, which has a very low backscatter coefficient. Accordingly, their gray levels are low, i.e. they appear dark.

Fig. 2b is the result of a process of binary segmentation on the image of Fig. 2a. In this process, pixels darker than an arbitrary gray level have been converted to zero brightness; those brighter than this level have been converted to the highest brightness level. The gray level selected as the boundary was chosen to best represent the outline of the pores as observed in the original micrograph. Thus, the black areas define the sizes and shapes of the pores on the plane of observation.

It is obvious from Fig. 2b that the pore shapes in hydrated cements are quite different from cylindrical pores assumed by the Washburn equation model. The pores are clearly not cylindrical, and the boundaries of most of them are visibly convoluted. Pore shapes in cement pastes were quantitatively evaluated by Wang and Diamond [10] using image analysis, and were found to have a high degree of convolution as measured by standard form factor measurements, and to be significantly elongated. Furthermore, Wang [11] found that the pore outlines exhibit appreciably fractal character when examined for this feature using a standard progressive dilation technique.

These departures of pore shape from that assumed in the model undoubtedly influence the output of MIP pore size distribution measurements. However, their effect ap-

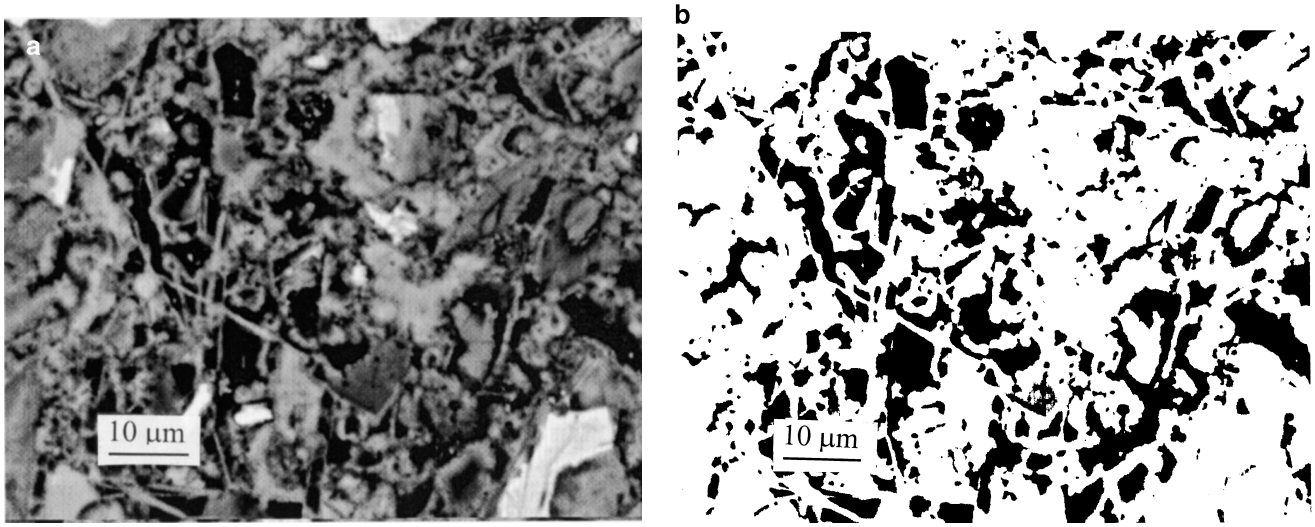

Fig. 2. (a) Backscatter SEM image showing representative area of a 7-day-old w:c 0.45 Portland cement paste. (b) Fig. 2 (a) after undergoing binary segmentation to show the pore space pixels as black and solid material pixels as fully white.

pears to be less important than the "accessibility effect" described below.

4. Pores in hydrated cement systems: accessibility of interior pores to the outer surface of the specimen

The Washburn equation [Eq. (1)] provides the means of calculating the pressure required to fill a cylindrical pore of a given cross-sectional diameter with mercury, *provided that mercury is accessible to that pore*. This issue of accessibility to mercury appears to be at the root of the failure of MIP to provide realistic pore size distributions.

The accessibility issue does not arise because individual pores may posses "ink-bottle" pore shapes, as occasionally stated in the literature (for example by Willis et al. [5]), but is far more fundamental than that. It arises from the fact that only a small proportion of the pores in hydrated cement specimens undergoing MIP is open directly to the outside of the specimen, i.e. is in contact with the surrounding mercury. Nearly all of the pores are in the interior of the specimen, and most of them can be reached by mercury only through a long percolative chain of intermediate pores of varying sizes and shapes.

The principle can be illustrated very simply. Fig. 3 provides two-dimensional drawings of two hypothetical arrangements of pores in a very short percolative chain consisting only of a single link. In Fig. 3a, a large cylindrical pore is open to the exterior of a specimen in contact with surrounding mercury. A second, smaller cylindrical pore opens to the larger pore. In an MIP measurement, the larger pore will fill with mercury when the pressure P_1 corresponding to its diameter is reached. The smaller pore will not fill at pressure P_1, but only when a higher pressure P_2 is reached that corresponds to its smaller diameter. A hypothetical pore system characterized by percolative chains that provide successively finer pores at each remove from the surface thus fulfills the requirements of the MIP model. Its mercury intrusion curve should be translatable to an appropriate pore size distribution curve. Unfortunately, such a pore system is highly unlikely to occur in hydrated cement systems.

On the other hand, Fig. 3b illustrates an equally simple arrangement which does not meet the requirements of the MIP model. In Fig. 3b, a small cylindrical pore is open to the outside. A second, larger cylindrical pore opens only to the smaller pore. The larger pore would fill with mercury at the relatively low pressure P_1 *if the mercury could reach it*. However, the geometry of the arrangement prevents

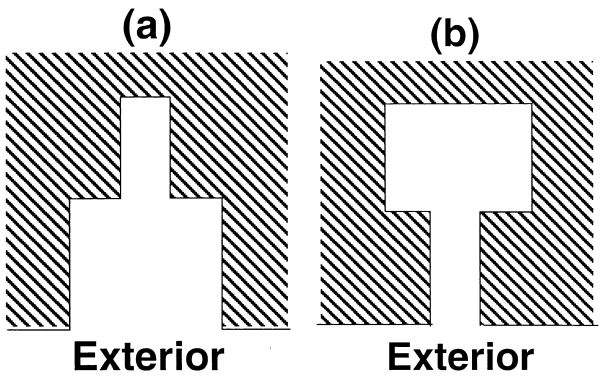

Fig. 3. (a) Illustrative diagram of a small cylindrical pore connected to the exterior of a specimen through a large cylindrical pore. Application of the Washburn equation model provides a correct tally of volume vs. pore diameter. (b) Illustrative diagram of a large cylindrical pore connected to the exterior of a specimen through a small cylindrical pore. Application of the Washburn equation model will record all of the volume at the diameter of the small pore, and the existence of the large diameter pore will not be detected.

this. The larger pore cannot fill until the higher pressure P_2 is reached that is needed to fill the smaller pore. When this pressure is reached, both pores will fill with mercury. Accordingly, the combined volumes of the two pores will be tallied at the high pressure step, and the volume of the large pore will be mistakenly allocated to the diameter of the small pore. A pore size distribution calculated from the Washburn equation thus provides no indication of the proportion of pore space constituted by the large pore, or indeed, of its very existence.

In typical mercury intrusion measurements, specimens of the order of 10 mm in size are ordinarily used; for example, Cook and Hover [7] used 13-mm cubes. Fig. 2 shows that cement pastes contain individual irregularly shaped pores in sizes up to ca. 10 μm. The percolative chains of such pores that must be traversed between the mercury surrounding the specimen and the middle of an uncracked specimen must include hundreds of steps. Each step provides an opportunity for the interfering action diagrammed in Fig. 3b.

On balance, one might expect from the above argument that employing specimens of smaller dimensions (i.e. having shorter percolative chains) might result in a shift to a coarser apparent pore structure. Such an effect was indeed found by Hearn and Hooton [12].

The occurrence of occasional "most favored" channels here and there within a specimen is certainly possible, in the vicinity of which the accessibility effect may be locally by-passed. Microcracks, bleeding channels, etc., may occur that mitigate the accessibility effect for some small proportion of the interior sample volume. This would be especially expected for mortars or concretes as compared to cement pastes.

The argument so far has not taken into account the specific character of the connectivity of pores within many hardened cement paste systems. The usual description of capillary pores in cement paste is that "they form an interconnected system randomly distributed throughout the cement paste" but that "in mature and dense pastes, the capillaries can become blocked by gel and segmented, so that they turn into capillary pores interconnected solely by gel pores" [13]. To the extent that this description is accurate, in mature cement pastes of reasonably low w:c ratio, the percolative chain is *necessarily* blocked by much finer connections at practically each step.

An equally strong argument can be made for the fraction of the pore space derived from hollow shell hydration grains, which in some places may be largely or entirely disconnected from percolative chains of capillary pores.

The concepts of pore blockage stated here are far from new. In 1970, Winslow and Diamond [14] noted that MIP curves of hardened cement paste all display an apparent 'threshold diameter' corresponding to a pressure above which very little intrusion into the specimen is recorded, and immediately below which the greatest portion of the intrusion takes place. This apparent threshold diameter is greater for higher water:cement ratios and for younger cement pastes; it reduces with age. The MIP plots of Cook and Hover [7], published in 1999, show this feature clearly; indeed, their MIP plots are quite similar to those reported in 1970 by Winslow and Diamond for pastes of corresponding age and w:c ratio.

To provide a numerical context, in the data of Winslow and Diamond [14] the threshold diameter for the 0.6 w:c paste decreased from about 0.30 μm at 1 day to about 0.04 μm at 7 days. For both w:c 0.4 and w:c 0.6 pastes, beyond 28 days, the threshold values were reduced to less than 0.02 μm. Similar trends are shown by Cook and Hover [7].

The significance of this feature of MIP plots for cement pastes was investigated by Winslow and Diamond [14]. Duplicate specimens were intruded at mercury pressures slightly less and slightly greater than the threshold pressure. After depressuring, the specimens were recovered, fractured, and the interior fractured surfaces thus exposed were immediately examined by optical microscopy. Specimens pressured to slightly less than the threshold pressure were recorded as being *light* gray in color. They displayed some "localized streams of mercury along the fractured cross-section of the interior; but also many local regions were present . . . with little observable evidence of penetration by mercury." In contrast, specimens pressured to slightly more than the threshold pressure were reported as being *dark* gray in color, and droplets of exuding mercury were found uniformly spaced over all regions exposed by the fracture. In the terminology of the present paper, a few interior areas within the specimen, for whatever reason, had access to mercury before the threshold pressure was reached. Most areas of the interior had access to mercury when and only when sufficient pressure was applied to overcome the accessibility effect.

Winslow and Diamond [14] also monitored the time rate at which mercury intruded their specimens at various pressures; in these measurements, a given pressure was maintained until intrusion ceased. In Fig. 4, the inverse rate of intrusion, i.e. the time needed to intrude a unit volume of mercury, is plotted as a function of the diameter attributed to the pressure step. Data for four different pastes are presented. The time to intrude a given volume of mercury was found to be very short at pressures significantly above and below the threshold pressure, but very long at pressures approximating to the threshold pressure. This slow movement of mercury into the specimen at the threshold pressure is additional evidence that movement of mercury from the exterior through long percolative chains of many steps is occurring at this pressure.

The picture inferred from this data is that in cement pastes, most interior pore spaces, regardless of pore size, are denied access to mercury until pressure is reached that effects a breakthrough. Then and only then can most pores fill, and they fill irrespective of their sizes (except for pores finer than the threshold diameter, which require additional pressure to fill). Such a filling process is vastly different

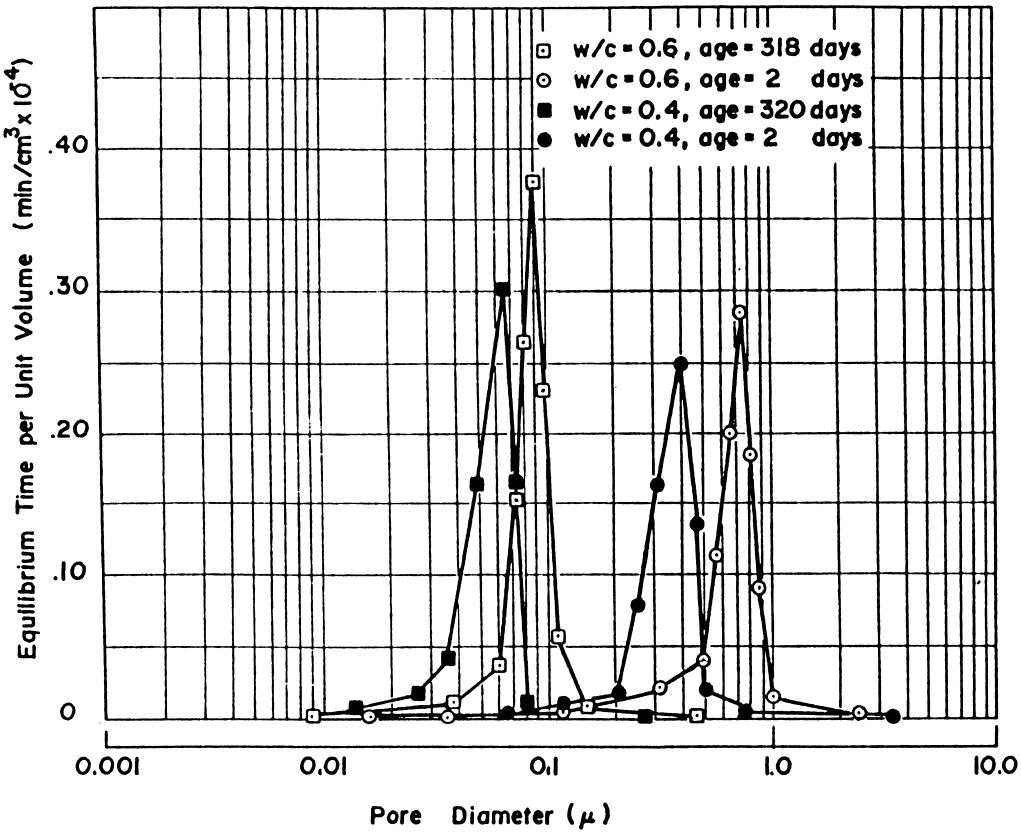

Fig. 4. Inverse rate of intrusion at each pressuring step in MIP, expressed as time (min) per unit volume of mercury intruded (cm^3). Note: each intrusion step was allowed to come to equilibrium. Data for 2-day-old and for mature w:c 0.6 and 0.4 cement pastes.

from that assumed by the Washburn equation model. Accordingly, application of the conventional MIP model to perfectly accurate mercury intrusion data *necessarily* leads to improper pore size distribution results, in which the bulk of the pore system is reported as sizes very much smaller than their actual sizes.

MIP curves for mortars and concretes show the same threshold phenomena, but in somewhat attenuated form. Typically, a modest but not negligible proportion of the total intrusion takes place at lower pressures before the threshold pressure is reached, and the threshold effect is not as sharply defined as it is in cement pastes. Presumably microcracks, bleeding channels, and other relatively unrestricted entryways enable a greater proportion of the interior space to be exposed to mercury at pressures less than the threshold pressure.

5. Pore sizes as examined directly vs. pore sizes derived from MIP measurements

The sizes of at least the larger pores in cement pastes and concretes can be viewed directly in optical microscopy; smaller pores can be seen in backscatter mode SEM, as shown in Fig. 1. In either case, "seeing" the pores of a given size leaves no doubt that pores of the size range seen do actually exist in the specimen being examined.

Fig. 5 consists of three separate parts. A representative backscatter SEM image of a 28-day-old w:c 0.40 cement paste taken at 1200 × is provided in Fig. 5a. Fig. 5b shows the same image, modified by the binary segmentation process as described for Fig. 1, so that only the pixels corresponding to the pores are retained, thus more clearly displaying the sizes and shapes of the pores.

Fig. 5c shows two MIP plots displayed for comparison with the micrograph. The curve to the right was obtained at Purdue University for the very same 28-day-old w:c sample that is represented in Fig. 5a. The other MIP curve was scaled by the writer from Fig. 7 of the Cook and Hover paper [7] for a cement paste specimen of the same age and w:c ratio. It should be noted that the *y* axes of the two MIP curves differ, one being expressed as cubic centimeters (cm^3) of mercury intruded per gram (g) of sample, the other, scaled from the Cook and Hover paper, as volume percent (vol.%) of the specimen.

The two MIP pore size distributions are quite similar; the one obtained at Purdue University allocates essentially all of the space to pores less than 0.15 μm in size; the other, slightly finer, allocates essentially all of the pores to sizes below about 0.07 μm. It is obvious that the ranges of pore

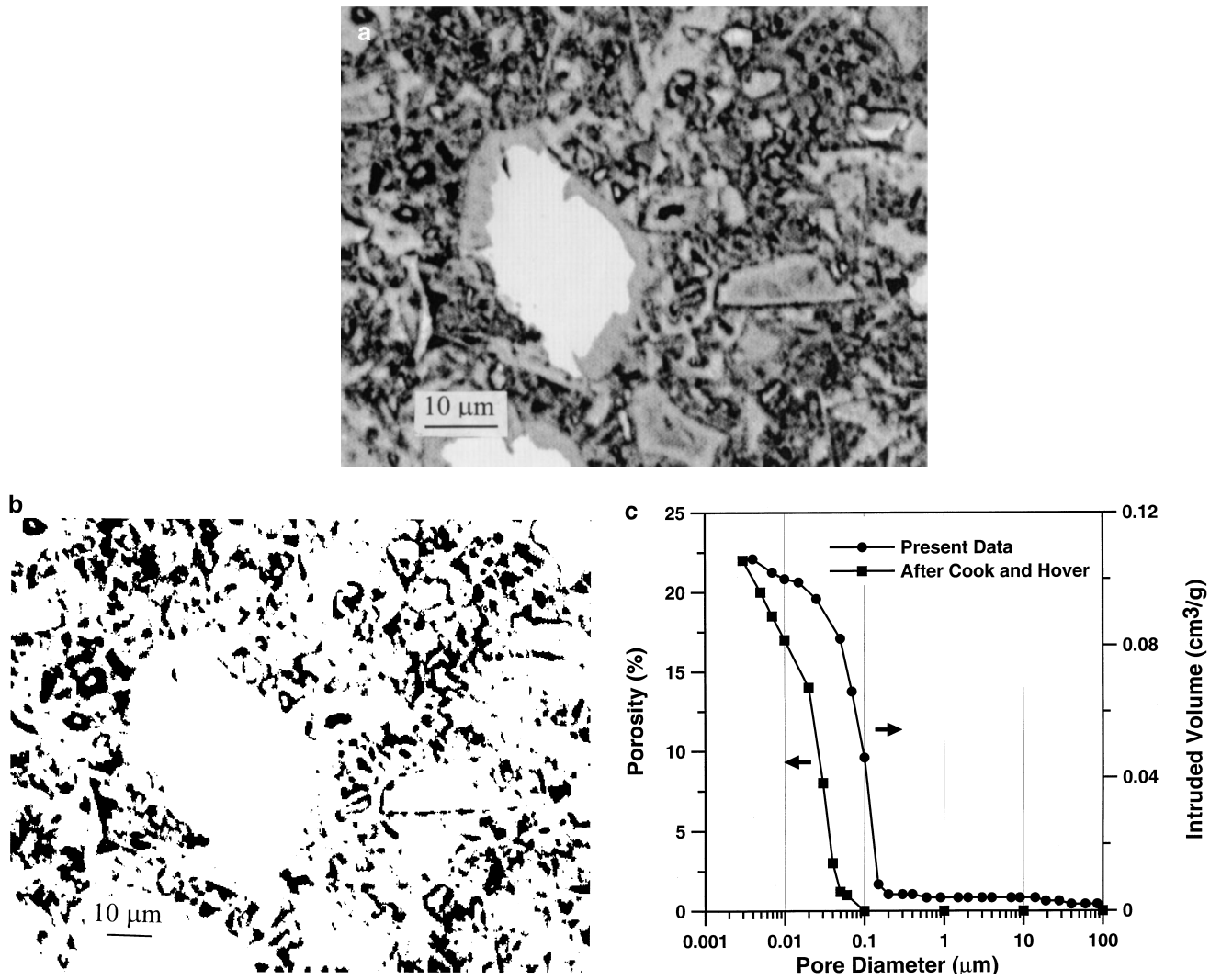

Fig. 5. (a) Backscatter SEM showing representative area of a 28-day-old w:c 0.40 Portland cement paste. (b) Fig. 5 (a) after undergoing binary segmentation to show the pore space pixels as black and solid material pixels as fully white. (c) Two MIP curves for 28-day-old w:c 0.40 Portland cement paste. Right-hand curve obtained at Purdue University for same paste specimen shown in Fig. 5 (a); left-hand curve redrawn from Cook and Hover [7] for a different cement paste of same age and w:c ratio.

sizes indicated by these MIP results in no way resemble the sizes of pores seen to be actually present in the micrograph of Fig. 5 in which the bulk of the visible pores are in the multi-micrometer size range.

A quantitative assessment of such differences was provided by Diamond and Leeman [15], who developed a procedure for quantitative pore size distribution measurement based on image analysis of backscatter SEM micrographs. In this work, a number of cement pastes of different w:c ratios were prepared using vacuum mixing (to avoid the inclusion of air voids). After hydration for various periods, the pastes were subjected both to MIP and to the image analysis pore size distribution measurement.

Fig. 6 provides a comparison for a vacuum-mixed 28-day-old w:c 0.40 paste. The image analysis pore size distributions is obviously incomplete, the lower bound of distinguishable pores being set by resolution limits at about 0.8 μm. The sizes measured by the image analysis extend up to ca. 10 μm. The MIP size distribution for the same paste tallies about twice the pore volume, *but almost all of it in sizes less than 0.2 μm*, i.e. smaller than the MIP threshold diameter of the sample.

6. The contributions of air voids to the MIP pore size distribution tally in ordinary pastes and mortars

It has been known for many years that air voids, in diameters varying from ca. 10 μm to the order of 500 μm are present in cement pastes, mortars, and concretes and constitute a substantial portion of the total pore volume. Air void size distributions in pastes were recently examined by Aligizaki and Cady [16] using a conventional stereoscopic optical microscope. The air void sizes found by these

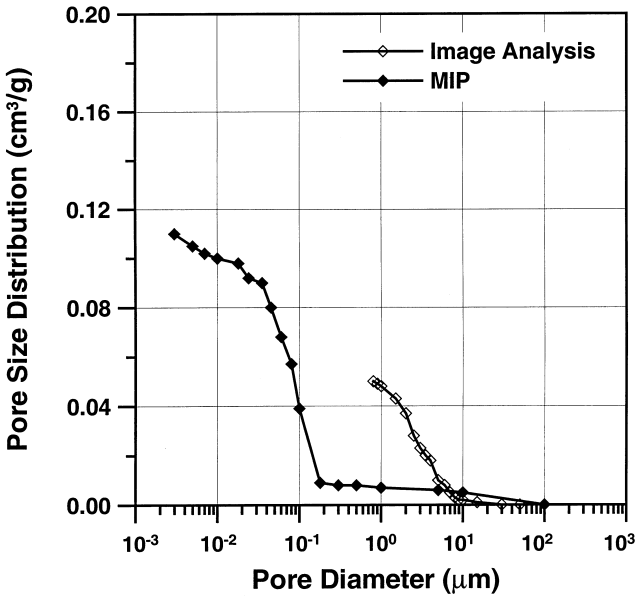

Fig. 6. Comparison of MIP and image analysis pore size distribution plots for the same vacuum-mixed 28-day-old w:c 0.40 cement paste.

authors ranged from about 150 μm down to about 10 μm, with occasional larger voids up to 450 μm being tallied. The air contents of the pastes varied between 1% and 2.5% by paste volume; this corresponds to between about 0.02 and about 0.05 cm^3/g. Air voids thus constitute a minor, but significant portion of the total pore volume of all cement pastes except those specially mixed under vacuum.

No indication that such air voids even exist in cement pastes (or mortars) is present in the many published MIP pore size distribution results examined by the writer.

Diamond and Leeman [15] prepared cement pastes with deliberately entrained air voids for comparison with otherwise identical vacuum-mixed pastes lacking air voids. Fig. 7 provides this comparison. The extra pore space introduced into the paste by incorporating air voids was easily detected by the image analysis pore size distribution measurement. The sizes of air voids tallied by image analysis were in the normal range as reported by Aligazaki and Cady [16], and the amount of "extra" air void pores was ca. 0.03 cm^3/g, also within the expected range of air void content for pastes as found by Aligazaki and Cady. The MIP results for this paste showed that intrusion into these air voids had taken place, as indicated by the appropriate amount of "extra" intrusion compared to the corresponding vacuum mixed pastes. However, as seen by comparing the MIP curves of Figs. 6 and 7, the extra space (i.e. the air voids) was not intruded by mercury until the threshold pressure was reached. The air voids were thus tallied as pores in the size range just below the threshold diameter, in this case, below about 0.20 μm.

The implication is that almost all published MIP size distributions of hydrated cement systems include the air void volume as part of the measured porosity, but "disguise" the air void space by not intruding the air voids until the threshold diameter pressure is reached. Image analysis pore size distributions, such as that plotted in Fig. 7, show the air void space tallied at appropriate diameters. While limited in size range, such distributions provide a more nearly true picture of the size distribution of pores (including air voids) as they actually exist in cement systems.

7. Reported results of Wood's metal intrusion

The recent investigation of Willis et al. [5] was previously mentioned as one of those reporting recent MIP results. However, the primary focus of these authors was not the MIP data, but rather, the investigation of the intrusion of molten Wood's metal into mortars under various pressures. Molten Wood's metal has a contact angle on hydrated cement that is similar to that of mercury, and these authors showed that its pressure–volume intrusion curve into a mortar was essentially identical to that of mercury into the same mortar. However, with Wood's metal, the pressure applied can be stopped at any given value, and if the sample is cooled, the location of the solidified Wood's metal within the specimen can be determined. Willis et al. [5] prepared sections of Wood's metal-intruded mortars for examination in backscatter SEM. They also carried out an image analysis size distribution determination of the pores filled with Wood's metal after pressuring to 5000 psi, this pressure being substantially higher than the threshold pressure, which was between 1000 and 1500 psi.

These authors reported that "at pressures below the threshold pressure Wood's metal was found in cracks and in large connected voids." and that "large voids that are not

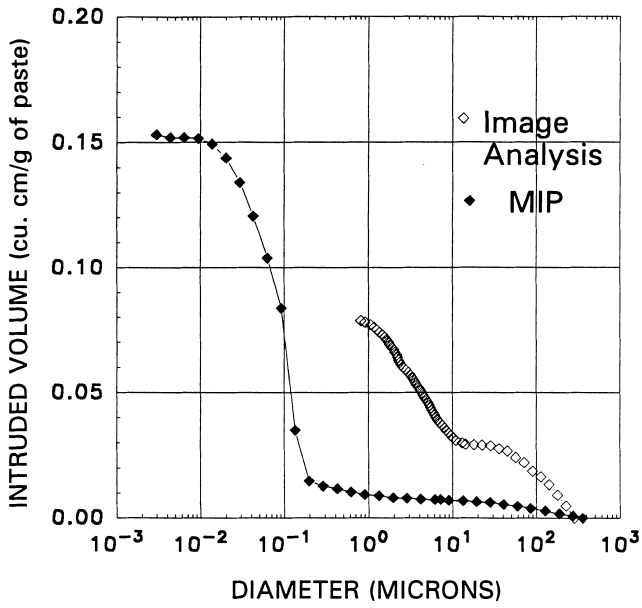

Fig. 7. Comparison of MIP and image analysis pore size distribution plots for 28-day-old w:c 0.40 cement paste containing air voids.

connected in the sample by these cracks remain unintruded.'' At 1000 psi, ''the crack penetration is pronounced and large connected voids are filled. The extremely porous region between closely spaced aggregate particles is also filled.'' These regions appear to constitute only a small portion of the paste in the mortar. The authors observed a dramatic difference in the appearance of the samples after exceeding the threshold pressure, i.e. at 1500 psi. They reported that ''a noticeable darkening of the entire sample occurred,'' and that ''all of the interfacial regions surrounding the aggregate are filled with metal and some of the groundmass has been intruded.''

In their Fig. 6, these authors presented a comparison of an MIP pore size distribution on an unintruded mortar specimen, with the pore size distribution determined by image analysis for the same sample fully intruded by Wood's metal at 5000 psi pressure. Willis et al. [5] presented their plots as volume vs. pore area, rather than the more common volume vs. pore diameter. The present writer has recalculated the data scaled from their Fig. 6 to pore diameter terms, and the recalculated data are shown in Fig. 8 of the present paper.

As indicated by Willis et al. [5], the MIP and image analysis tally the same total pore space, about 9% of the sample volume. This may be fortuitous, since in carrying out the image analysis, areas containing air voids were apparently excluded from examination [17]. The intrinsic non-air void pores, shown to be present by virtue of their being filled with Wood's metal, are mostly in sizes between 1 and 10 μm, similar to the size range found in the previous image analysis results reported in the present paper. In contrast, the MIP results suggest incorrectly that virtually

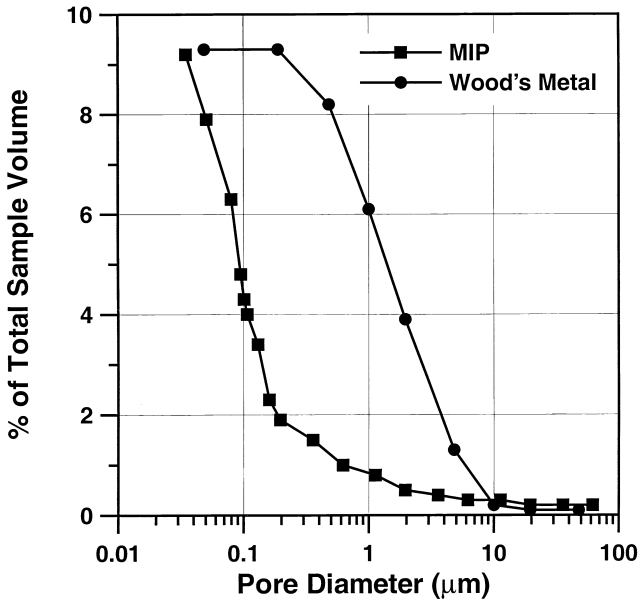

Fig. 8. Comparison of plots of image analysis size distribution of Wood's metal-filled pores and MIP results for the same 14-day-old w:c mortar (after Willis et al. [5]).

the entire pore volume is in sizes finer than 0.20 μm, i.e. there is virtually no overlap between the sizes indicated by MIP and the sizes shown to be present in the examination of the Wood's metal specimens.

8. Threshold diameter and total intrusion as indexes of pore structure

MIP size distribution plots have often been used in a way that does not necessarily depend on the actual distribution of pore sizes as such. Instead, values of the threshold diameter and of the total volume of intruded mercury are taken as indexes of the pore structure for comparison with pore structures of other pastes or mortars.

The threshold diameter would appear to be a useful index of the comparative size of ''choke points'' between percolative steps in the intrusion of mercury under pressure. To the extent that the intrusion process at the specific pressure involves only Darcy flow through restrictions (and not crushing of the restricting areas), the threshold diameter would seem to be a valid comparative parameter, related to permeability and ion diffusion in cement systems.

The total volume of pore space intrudable by mercury may also be useful, as a comparative index of the porosity of the system. Intrudable volume varies with w:c ratio and age in much the same way as threshold diameter. It should be understood that intrudable volume includes air voids as well as intrinsic paste pores, and the air void content may fluctuate depending on mixing procedure. It should be noted that intrudable porosity as measured in MIP is not a measure of total porosity in the system. In addition to the pore space actually intruded by mercury, finer pores (gel pores?) undoubtedly exist in cement pastes that require pressure for entry beyond the pressuring capacity of commercial instrumentation. Some completely isolated pores that are entirely sealed against intrusion may be present as well.

9. Conclusions

Evidence has been presented that MIP measurements of pore size distribution systematically misallocates the sizes of almost all of the volume of pores in hydrated cementitious materials, and assigns then to sizes smaller that of the threshold diameter regardless of their actual sizes. It appears that the failure of the MIP method with cement systems is intrinsic rather than accidental, and derives from the lack of direct accessibility of most of the pore volume (including air voids) to the mercury surrounding the specimen.

Air voids, present in pastes unless they are vacuum-mixed, are intruded after the threshold pressure is reached, and are not generally recognized as such in the MIP plots.

If a measurement method does not properly measure the parameter that it attempts to measure by as large a margin as MIP appears to do in cement systems, it is appropriate to

consider discarding it. It seems inescapable to the writer that MIP should be discarded *as a method of measuring pore size distributions* in hydrated cement systems.

However, knowledge of the threshold diameter and of the intrudable pore volume may constitute useful comparative indexes of the cement paste or concrete pore. These can be determined by MIP equipment without reference to any calculated size distribution. Such MIP applications do appear to be valid within the limitations imposed by the nature of the mercury intrusion experiment.

Acknowledgments

Helpful discussions with J. Olek and D.L. Lange are acknowledged with thanks. The writer is indebted to Professor Emeritus D.N. Winslow and to more recent former students Mark E. Leeman and Yuting Wang. The opinions expressed, however, are entirely his own.

References

[1] J.M. Khatib, S. Wild, Sulfate resistance of metakaolin mortar, Cem Concr Res 28 (1) (1998) 83–92.
[2] B. Zhang, Relationship between pore structure and mechanical properties of ordinary concrete under bending fatigue, Cem Concr Res 28 (5) (1998) 699–712.
[3] L. Bagel, Strength and pore structure of ternary blended cement mortars containing blast furnace slag and silica fume, Cem Concr Res 28 (7) (1998) 1011–1022.
[4] V. Kanna, R.A. Olson, H.M. Jennings, Effect of shrinkage and moisture content on the physical characteristics of blended cement mortars, Cem Concr Res 28 (10) (1998) 1467–1477.
[5] K.L. Willis, A.B. Abell, D.A. Lange, Image-based characterization of cement pore structure using Wood's metal intrusion, Cem Concr Res 28 (12) (1998) 1695–1706.
[6] A. Loukili, A. Khelidj, P. Richard, Hydration kinetics, change of relative humidity, and autogenous shrinkage of ultra-high-strength concrete, Cem Concr Res 29 (4) (1999) 577–584.
[7] R.A. Cook, K.C. Hover, Mercury porosimetry of hardened cement pastes, Cem Concr Res 29 (6) (1999) 933–944.
[8] F. Puerta, M.T. Blanco-Varela, T. Vazquez, Behavior of cement mortars containing an industrial waste from aluminum refining: stability in $Ca(OH)_2$ solutions, Cem Concr Res 29 (10) (1999) 1673–1680.
[9] D. Shi, D.N. Winslow, Contact angle and damage during mercury intrusion into cement pastes, Cem Concr Res 15 (4) (1985) 645–654.
[10] Y. Wang, S. Diamond, An approach to quantitative image analysis for cement pastes, in: S. Diamond, S. Mindess, F.P. Glasser, L.W. Roberts, J.P. Skalny, L.D. Wakeley (Eds.), Microstructure of Cement Based Systems/Bonding and Interfaces in Cementitious Materials, Mater Res Soc Proc Vol. 370, (1995) 23–32 Pittsburgh.
[11] Y. Wang, Microstructural study of hardened cement paste by backscatter scanning electron microscopy and image analysis, PhD thesis, Purdue University, 1995.
[12] N. Hearn, R.D. Hooton, Sample mass and dimension effects on mercury intrusion porosimetery results, Cem Concr Res 22 (5) (1992) 970–980.
[13] A.M. Neville, Properties of Concrete, 4th edn., Wiley, New York, 1996, p. 32.
[14] D.N. Winslow, S. Diamond, A mercury porosimetry study of the evolution of porosity in portland cement, J Mater (ASTM) 5 (1970) 564.
[15] S. Diamond, M.E. Leeman, Pore size distributions in hardened cement paste by image analysis, in: S. Diamond, S. Mindess, F.P. Glasser, L.W. Roberts, J.P Skalny, L.D. Wakeley (Eds.), Microstructure of Cement Based Systems/Bonding and Interfaces in Cementitious Materials, Mater Res Soc Proc Vol. 370, (1995) 217–226 Pittsburgh.
[16] K.K. Aligazaki, P.D. Cady, Air content and size distribution of air voids in hardened cement pastes using the thin section-analysis method, Cem Concr Res 29 (2) (1999) 273–280.
[17] D. Lange, personal communication, Oct. 1999.